An engineered Calvin-Benson-Bassham cycle for carbon dioxide fixation in Methylobacterium extorquens AM1

von Borzyskowski, Lennart Schada; Carrillo, Martina; Leupold, Simeon; Glatter, Timo; Kiefer, Patrick; Weishaupt, Ramon; Heinemann, Matthias; Erb, Tobias J

Published in:
Metabolic Engineering

DOI:
10.1016/j.ymben.2018.04.003

Publication date:
2018

Metabolic Engineering 47 (2018) 423–433

Contents lists available at ScienceDirect

Metabolic Engineering

journal homepage: www.elsevier.com/locate/meteng

An engineered Calvin-Benson-Bassham cycle for carbon dioxide fixation in *Methylobacterium extorquens* AM1

Lennart Schada von Borzyskowski[a,b], Martina Carrillo[a], Simeon Leupold[d], Timo Glatter[a], Patrick Kiefer[b], Ramon Weishaupt[b,1], Matthias Heinemann[d], Tobias J. Erb[a,c,*]

[a] Max Planck Institute for Terrestrial Microbiology, Department of Biochemistry and Synthetic Metabolism, Karl-von-Frisch-Straße 10, 35043 Marburg, Germany
[b] Institute of Microbiology, ETH Zurich, Vladimir-Prelog-Weg 4, 8093 Zurich, Switzerland
[c] SYNMIKRO, LOEWE Center for Synthetic Microbiology, Universität Marburg, 35043 Marburg, Germany
[d] Molecular Systems Biology, Groningen Biomolecular Sciences and Biotechnology Institute, University of Groningen, Nijenborgh 4, 9747 AG Groningen, The Netherlands

ARTICLE INFO

Keywords:
Calvin-Benson-Bassham cycle
Carbon fixation
Methylobacterium extorquens AM1
RuBisCO
Methylotrophy
Autotrophy

ABSTRACT

Organisms are either heterotrophic or autotrophic, meaning that they cover their carbon requirements by assimilating organic compounds or by fixing inorganic carbon dioxide (CO_2). The conversion of a heterotrophic organism into an autotrophic one by metabolic engineering is a long-standing goal in synthetic biology and biotechnology, because it ultimately allows for the production of value-added compounds from CO_2. The heterotrophic Alphaproteobacterium *Methylobacterium extorquens* AM1 is a platform organism for a future C1-based bioeconomy. Here we show that *M. extorquens* AM1 provides unique advantages for establishing synthetic autotrophy, because energy metabolism and biomass formation can be effectively separated from each other in the organism. We designed and realized an engineered strain of *M. extorquens* AM1 that can use the C1 compound methanol for energy acquisition and forms biomass from CO_2 by implementation of a heterologous Calvin-Benson-Bassham (CBB) cycle. We demonstrate that the heterologous CBB cycle is active, confers a distinct phenotype, and strongly increases viability of the engineered strain. Metabolic ^{13}C-tracer analysis demonstrates the functional operation of the heterologous CBB cycle in *M. extorquens* AM1 and comparative proteomics of the engineered strain show that the host cell reacts to the implementation of the CBB cycle in a plastic way. While the heterologous CBB cycle is not able to support full autotrophic growth of *M. extorquens* AM1, our study represents a further advancement in the design and realization of synthetic autotrophic organisms.

1. Introduction

All cellular life forms need to assimilate carbon for the synthesis of organic molecules that comprise their biomass. This fundamental feature of life is achieved by one of two distinct metabolic modes: Heterotrophy, i.e., the assimilation of reduced organic carbon compounds, or autotrophy, i.e., the fixation of inorganic carbon dioxide (CO_2) into biomass. The latter process is typically energized by light (photo-autotrophy) or chemical energy (chemo-autotrophy).

In the past, biotechnology has mainly capitalized on heterotrophic metabolism for the production of value-added chemicals from simpler carbon compounds, such as sugars or amino acids (Dellomonaco et al., 2011; Enquist-Newman et al., 2014; Galanie et al., 2015; Paddon et al., 2013). The direct utilization of CO_2 as carbon feedstock in biotechnology, however, has gained considerable interest recently. Metabolic engineering of autotrophs could create novel routes that allow the direct conversion of CO_2 into valuable chemicals (Bar-Even et al., 2010; Liu et al., 2016; Nichols et al., 2015; Schwander et al., 2016). When coupled to photosynthesis, hydrogen gas, reduced chemical compounds or electricity, these routes would not only provide a sustainable carbon capture and conversion strategy for biotechnology, but also circumvent the need for organic carbon from plant biomass, with its low photosynthetic efficiency (typically < 1%) and ethical concerns as it directly competes with food production (Fargione et al., 2008; Sims et al., 2010).

For production of value-added compounds from CO_2, two different approaches can be envisioned. One approach is the implementation of biosynthetic production pathways into naturally existing carbon-fixing organisms, such as cyanobacteria and algae. The other option is to convert a conventional heterotrophic production strain into a 'synthetic

* Corresponding author at: Max Planck Institute for Terrestrial Microbiology, Department of Biochemistry and Synthetic Metabolism, Karl-von-Frisch-Straße 10, 35043 Marburg, Germany.
E-mail address: toerb@mpi-marburg.mpg.de (T.J. Erb).
[1] Present Address: Laboratory for Biointerfaces, Empa, Swiss Federal Laboratories for Materials Science and Technology, Lerchenfeldstrasse 5, 9014 St. Gallen, Switzerland.

https://doi.org/10.1016/j.ymben.2018.04.003
Received 18 July 2017; Received in revised form 21 March 2018; Accepted 2 April 2018
Available online 04 April 2018

autotroph'. Compared to the first approach, the latter strategy is more radical. Implementing autotrophy into a native heterotroph requires a complete remodeling of its central carbon and energy metabolism, which is comparable to a 'metabolic heart transplantation' (Bar-Even et al., 2010). Therefore, the successful realization of a 'synthetic autotroph' will be a milestone in synthetic biology that probes the plasticity and modularity of metabolism to realize a 'plug-and-play principle' in living organisms.

Previous attempts of engineering a synthetic autotrophic organism largely focused on the model bacterium *Escherichia coli*. In a pioneering study, all enzymes of the 3-hydroxypropionate bicycle for CO_2 fixation were functionally expressed in *E. coli*. However, neither autotrophic growth nor a CO_2-fixing phenotype of the engineered strain was achieved (Mattozzi et al., 2013). Other groups have focused on implementing the Calvin-Benson-Bassham cycle (CBB cycle) for CO_2 fixation in this organism. Overexpression of the CBB cycle's key enzymes, ribulose-1,5-bisphosphate carboxylase/oxygenase (RuBisCO) and phosphoribulokinase (Prk) in *E. coli* resulted in a significant reduction of CO_2 emissions (Zhuang and Li, 2013), and even allowed the biosynthesis of sugars from CO_2 (Antonovsky et al., 2016). Although these studies represent important steps towards realizing 'synthetic autotrophy', all CO_2-fixing *E. coli* strains created so far still depend on addition of a multi-carbon compound that is produced from biomass feedstocks.

Here, we sought to move one step further by engineering an organism that is able to satisfy its needs for energy and biomass solely from single-carbon sources that are not derived from plant feedstocks. To this end, we chose the Alphaproteobacterium *Methylobacterium extorquens* AM1 (Peel and Quayle, 1961) as chassis organism. This pink-pigmented, aerobic organism can grow heterotrophically on multi-carbon compounds as well as on the reduced single carbon compound methanol. Methanol is projected to play a key role in future bioeconomies (Bertau et al., 2014; Olah, 2013; Schrader et al., 2009), and *M. extorquens* AM1 is considered a biotechnological platform organism of the future. Several tools for genetic and metabolic engineering of *M. extorquens* AM1 are available (Choi et al., 2006; Chubiz et al., 2013; Marx, 2008; Marx and Lidstrom, 2001, 2002, 2004; Schada von Borzyskowski et al., 2015) and different *Methylobacterium* strains have already been developed to produce value-added chemicals from methanol (Hofer et al., 2010; Hu and Lidstrom, 2014; Ochsner et al., 2015; Orita et al., 2014; Sonntag et al., 2014, 2015a, 2015b). Expanding the metabolic capacity of *M. extorquens* AM1 to form biomass from the ubiquitous raw material CO_2, while using the highly reduced energy carrier methanol solely as an electron source, is a plausible and highly desirable goal.

In this study, we established a heterologous CBB cycle for CO_2 fixation in *M. extorquens* AM1. We engineered the central carbon metabolism of *M. extorquens* AM1 to separate energy acquisition from biomass formation. In our engineered strain, electrons are provided from methanol oxidation, while biomass is formed by CO_2 fixation via the heterologous CBB cycle. We demonstrate operation of the heterologous CBB cycle by growth phenotyping, ^{13}C-tracer analysis, and whole-cell proteomics. Our results reveal a positive phenotype upon expression of the CBB cycle as well as significant metabolic and proteomic changes in the engineered strain. Our work represents a stepping stone towards creating a fully synthetic autotrophic organism.

2. Material and methods

2.1. Bacterial strains, culture conditions, and plasmid delivery

If not mentioned otherwise, wild-type (WT) *M. extorquens* AM1 (Peel and Quayle, 1961) was used. *E. coli* DH5α was used for construction and amplification of all plasmids used in this work. *M. extorquens* AM1 was cultured at 30 °C in minimal medium (Peyraud et al., 2009) supplemented with either 124 mM methanol or 30.8 mM succinate, or in Nutrient Broth (NB) without additional NaCl (Sigma-Aldrich, St. Louis, MO, USA). *E. coli* DH5α was cultured in LB medium at 37 °C. When appropriate, media were supplemented with tetracycline or kanamycin at a concentration of 10 or 50 μg mL^{-1}, respectively. Competent cells of *M. extorquens* AM1 WT and all mutant strains were made according to a published procedure, and electroporation was used for plasmid delivery into *M. extorquens* AM1 as described previously (Toyama et al., 1998).

2.2. Plasmid construction

All oligonucleotides used in this study are listed in SI Table 1. All plasmids used and created in this study are listed in SI Table 2. Cloning was performed according to standard protocols (Sambrook and Russell, 2001). Restriction enzymes and T4 DNA ligase were obtained from NEB (Frankfurt am Main, Germany). FastAP thermosensitive alkaline phosphatase was obtained from Thermo Scientific (St. Leon-Rot, Germany). PCRs were conducted with Phusion polymerase (Thermo Scientific, St. Leon-Rot, Germany) following the recommendations of the manufacturer using the protocol for GC-rich templates. Correct plasmid sequences were verified by Sanger sequencing (Eurofins, Ebersberg, Germany).

pCM80 (Marx and Lidstrom, 2001) was cut with *Bam*HI and *Eco*RI, the PCR product of RuBisCO (amplified from genomic DNA of *Rhodospirillum rubrum* S 1 with the primers R_Rbc_fw and R_Rbc_rv) was digested with the same enzymes and ligated into the dephosphorylated vector backbone to generate pTE92. pTE92 was cut with *Hind*III and *Bam*HI, the PCR product of Prk from *Methylobacterium extorquens* AM1 (generated with primers M_Prk_fw and M_Prk_rv) was digested with the same enzymes and ligated into the dephosphorylated vector backbone to generate pTE94. pTE95 was generated by site-directed mutagenesis using pTE94 as template and the primers K191M_QC_fw and K191M_QC_rv. Prk was PCR-amplified from genomic DNA of *Synechococcus elongatus* PCC 7942 with the primers S_Prk_fw and S_Prk_rv. The resulting PCR product was digested with *Hind*III and *Bgl*II and ligated into pTE92 that had been digested with *Hind*III and *Bam*HI to generate pTE96.

The large and small subunits of RuBisCO (RuBisCO LSU + SSU) as well as Prk were PCR-amplified from genomic DNA of *Paracoccus denitrificans* DSM 413 with the primers P_RbcL_fw, P_RbcL_rv, P_RbcS_fw, P_RbcS_rv, P_Prk_fw and P_Prk_rv respectively. The PCR products were digested with *Nde*I and *Eco*RI and ligated into pET28b that had been digested with the same enzymes to generate pTE245, pTE246, and pTE248, respectively. The three His-tagged ORFs were excised from these vectors with *Xba*I and *Eco*RI and ligated into pTE100 that had been digested with *Xba*I and *Mun*I to generate pTE500, pTE502, and pTE504. His-tagged Rbc LSU was excised from pTE500 with *Xba*I and *Kpn*I and ligated into pTE102 that had been digested with *Spe*I and *Kpn*I to generate pTE519. His-tagged Prk was excised from pTE504 with *Xba*I and *Kpn*I and ligated into pTE519 that had been digested with *Spe*I and *Kpn*I to generate pTE535. His-tagged Rbc SSU was excised from pTE502 with *Xba*I and *Kpn*I and ligated into pTE535 that had been digested with *Spe*I and *Kpn*I to generate pTE550.

The flanking regions of *glyA* from *M. extorquens* AM1 were PCR-amplified with the primers glyA_up_fw, glyA_up_rv, glyA_do_fw and glyA_do_rv. The PCR products of the up- and downstream regions were used as templates to generate a fusion PCR product by overlap PCR with the primers glyA_up_fw and glyA_do_rv. The overlap PCR product was digested with *Eco*RI and *Xba*I and ligated into pK18-mob-sacB (Schäfer et al., 1994), which had been digested with the same enzymes, to generate pTE210.

2.3. Strain construction

All strains used and created in this study are listed in SI Table 2. *M. extorquens* AM1 Δ*glyA* was made from *M. extorquens* AM1 WT by

transforming pTE210 into electrocompetent cells and screening for kanamycin resistance and sucrose sensitivity. The deletion was confirmed by diagnostic PCR and sequencing of the PCR product.

M. extorquens AM1 Δ*cel* Δ*ftfL*::Kan was made from *M. extorquens* AM1 Δ*cel* (strain CM2720) (Delaney et al., 2013) by introduction of the *ftfL* deletion using pCM216 (Marx et al., 2003). The transformants were screened for kanamycin resistance and tetracycline sensitivity. The deletion was confirmed by diagnostic PCR and sequencing of the PCR product.

2.4. Cell lysis and determination of protein concentration

M. extorquens AM1 cultures were harvested in mid-exponential phase and aliquoted in 400 mg samples in 800 µL 100 mM Tris pH 7.8. Cells were lysed by sonication on ice with a Sonopuls HD 200 sonicator (Bandelin, Berlin, Germany), using 30% of the maximal amplitude for 15 s, which was repeated 5 times. The samples were centrifuged at 40,000 g and 4 °C for 60 min and the supernatant was transferred into new tubes. The total protein concentration of the supernatant was quantified by Bradford assay (Bradford, 1976) with bovine serum albumin (BSA) as standard and analyzed on 12.5% SDS PAGE gels (Laemmli, 1970), applying 20 µg protein per lane.

2.5. Spectrophotometric assays to measure RuBisCO and Prk activities

The activity of RuBisCO in cell-free extracts was measured by a continuous spectrophotometric assay determining NADH absorption at 340 nm on a Cary 50 UV/Vis spectrophotometer at 30 °C according to published procedures (Racker, 1957, 1962). The cell-free extract of a pCM80 transformant was used to correct for the background reaction in all assays. The activity of Prk in cell-free extracts was measured by modifying the same assay, using 0.6 mM ribulose 5-phosphate as substrate for Prk and adding purified RuBisCO from *R. rubrum* S 1 (a kind gift from Ryan Farmer and Bob Tabita, Ohio State University) in excess, so that activity of Prk could be measured by coupling it to the downstream reaction of RuBisCO.

2.6. Growth assays

2.6.1. Assays in 96-well plates

All strains of *M. extorquens* AM1 were pre-grown at 30 °C in minimal medium containing succinate as sole carbon source until an OD_{600} of approximately 1.5. Then, cells were harvested, washed with minimal medium containing methanol and used to inoculate growth cultures of 180 µL minimal medium containing methanol in 96-well plates (Nunclon Delta Surface, Thermo Fisher Scientific, Darmstadt, Germany) sealed with parafilm. Growth at 30 °C was monitored in at least three technical replicates and at least two biological replicates at 600 nm in a Tecan Infinite M200Pro reader connected to a Tecan Gas Control Module (Tecan, Männedorf, Switzerland). Data was analyzed using the GraphPad Prism 6 software.

2.6.2. Assays in bioreactor

M. extorquens AM1 Δ*cel* Δ*ftfL*::Kan pTE94 was pre-grown at 30 °C in 200 mL minimal medium containing succinate as sole carbon source in an atmosphere with 5% CO_2 until an OD_{600} of approximately 1.5. Then, cells were harvested, washed with minimal medium containing methanol and used to inoculate a DASGIP SR0700ODLS bioreactor (Eppendorf, Hamburg, Germany) to an initial OD_{600} of approximately 0.2. During assembly of the bioreactor, all parts and tubes were rinsed with methanol and water in order to avoid contamination with ethanol and other substances. The bioreactor contained an initial volume of 700 mL, was stirred at 500 rpm and continuously gassed with 5% CO_2 in air at a flow rate of 15 L h^{-1}. pH was kept constant at 7.0 by addition of 3 M NH_4OH and 1 M H_2SO_4, and temperature was kept at 30 °C. Samples were taken via the sampling port of the bioreactor and OD_{600} was measured manually on a Ultrospec 3000 photospectrometer (Pharmacia Biotech (now part of GE Healthcare), Uppsala, Sweden).

2.7. Quantification of CFU/mL

Four replicate cultures each of *M. extorquens* AM1 Δ*cel* Δ*ftfL*::Kan pTE94 and pTE95 were pre-grown at 30 °C in minimal medium containing succinate as sole carbon source in an atmosphere with 5% CO_2 until an OD_{600} of approximately 1.5. Then, cells were harvested, washed with minimal medium containing methanol, and used to inoculate cultures of 25 mL minimal medium containing methanol to an OD_{600} of 0.2, which were incubated in an atmosphere with 5% CO_2. Every 50 h and also 8 h after inoculation, samples were taken. Dilution series of these samples were spread on plates (1.5% agar) containing minimal medium with 30.8 mM succinate and tetracycline and incubated for 96 h at 30 °C, after which the resulting colonies were counted manually.

2.8. ^{13}C-tracer analysis-based metabolomics

Cultures of *M. extorquens* AM1 Δ*cel* Δ*ftfL*::Kan pTE94 and pTE95 were pre-grown at 30 °C in minimal medium containing succinate as sole carbon source in an atmosphere with 5% CO_2 until the late exponential phase. Then, cells were harvested, washed with minimal medium containing methanol and used to inoculate cultures of 30 mL minimal medium containing methanol. The cultures were incubated for 4 h in a defined atmosphere with 5% CO_2 at natural ^{13}C abundance. These cultures were then quickly collected by centrifugation (1 min, 10,000 g), the supernatant was discarded, and the pellet was washed with 30 mL medium (pre-warmed to 30 °C) containing no carbon source. The cultures were again pelleted (1 min, 10,000 g), the supernatant was discarded, and cells were re-suspended in 30 mL fresh medium containing either 124 mM ^{13}C-methanol or 8 mM ^{13}C-bicarbonate and 124 mM methanol at natural ^{13}C abundance. Cultures were then transferred into 100 mL shake flasks and incubated in an atmosphere containing 5% CO_2 at natural ^{13}C abundance when containing ^{13}C-methanol or incubated in a VLSB18 shaking water bath (VWR, Darmstadt, Germany) kept at 30 °C when containing ^{13}C-bicarbonate. This marked the starting point of the labeling experiment. To analyze the dynamic labeling process of metabolites, samples were taken after 0, 1, 5, 10, 15, 30, 45, 60 and 90 min. In short, each sample was transferred onto a polyethersulfone (PESU) 0.2 µm filter (Sartorius Stedim, Göttingen, Germany) pre-washed with an excess amount of 60 °C hot water. By applying vacuum, the medium was removed and the cells were washed with 5 mL 30 °C warm MilliQ water. The filter with cells was transferred into 100 mL Schott bottles filled with 8 mL of − 20 °C cold quenching solution (60% acetonitrile/20% methanol/20% 0.5 M formic acid) and kept on ice for 15 min. The bottles were sonicated every 5 min for 20 s using a Bransonic M2800-E sonication bath (VWR, Darmstadt, Germany). Afterwards, the filters were removed, samples were transferred into prepared 50 mL falcon tubes, frozen in liquid nitrogen, and lyophilized overnight. Sampled biomass amount was approximately 1 mg of cell dry weight.

Lyophilized samples were resuspended in MilliQ water to give a final biomass concentration of 1 µg/µL. The resuspended samples were centrifuged at 20,000 g for 15 min at 4 °C to remove insoluble particles. Prior to HPLC-MS analysis, 10 µL of each sample was mixed with 90 µL of solvent A (see below).

Nanoscale ion-pair reversed phase HPLC–MS analysis of the resuspended samples was performed as described previously (Müller et al., 2015), with the following modifications. Solvent A was 233 µM tributylamine in 234 µM acetic acid adjusted to pH 9.0 with NH_4OH; subsequently, 3% methanol were added to the solution. Solvent B was a 1:1 (V:V) mixture of 2-propanol and methanol. The applied gradient was as follows: 0 min (A 100%, B 0%); 3 min (A 100%, B 0%); 35 min (A 88%, B 12%), 36 min (A 10%, B 90%), 48 min (A 10%, B 90%), 49 min (A 100%, B 0%), 60 min (A 100%, B 0%). The flow rate was kept

constant at 400 µL/min throughout the gradient.

Obtained MS-data were analyzed using eMZed 2.24.6 (Kiefer et al., 2013; emzed.ethz.ch).

2.9. Whole-cell shotgun proteomics using liquid chromatography-mass spectrometry (LC-MS/MS)

Four replicate cultures each of *M. extorquens* AM1 Δ*cel*, Δ*cel* pTE94, Δ*cel* Δ*ftfL*::Kan pTE94 and Δ*cel* Δ*ftfL*::Kan pTE95 were pre-grown at 30 °C in minimal medium containing succinate as sole carbon source in an atmosphere with 5% CO_2 until the late exponential phase. At this point, the first samples for proteomic analysis were taken. Then, cells were harvested, washed with minimal medium containing methanol and used to inoculate cultures of 200 mL minimal medium containing methanol, to an OD_{600} of approx. 0.2 and incubated in an atmosphere with 5% CO_2. After a sufficient incubation time (20 h for both of the Δ*cel* strains, 65 h for both of the Δ*cel* Δ*ftfL* strains) with these carbon sources, samples for proteomic analysis were taken. Samples were washed once with ice-cold PBS and cell pellets were flash-frozen in liquid nitrogen and stored at − 80 °C until further processing.

Sample preparation was carried out as described previously (Glatter et al., 2015), with the following modifications: 2% sodium lauroyl sarcosinate (SLS) was used instead of 2% sodium deoxycholate (SDC), and quenching with N-acetylcysteine as well as digestion with LysC were omitted.

LC-MS/MS analysis of digested lysates was performed on a Thermo QExactive Plus mass spectrometer (Thermo Scientific), which was connected to an electrospray ionsource (Thermo Scientific). Peptide separation was carried out using an Ultimate 3000 RSLCnano (Thermo Scientific) equipped with a RP-HPLC column (75 µm x 35 cm) packed in-house with C18 resin (1.9 µm; Dr. Maisch). The following separating gradient was used: 98% solvent A (0.15% formic acid) and 2% solvent B (80% acetonitrile, 0.15% formic acid) to 32% solvent B over 175 min and to 50% B for additional 20 min at a flow rate of 300 nl/min. The data acquisition mode was set to obtain one high resolution MS scan at a resolution of 70,000 full width at half maximum (at *m/z* 200) followed by MS/MS scans of the 10 most intense ions. To increase the efficiency of MS/MS attempts, the charged state screening modus was enabled to exclude unassigned and singly charged ions. The dynamic exclusion duration was set to 30 s. The ion accumulation time was set to 50 ms (MS) and 50 ms at 17,500 resolution (MS/MS). The automatic gain control (AGC) was set to 3×10^6 for MS survey scan and 1×10^5 for MS/MS scans.

Label-free quantification of raw data and data evaluation was performed as described previously (Ahrné et al., 2013; Glatter et al., 2015). In short, the raw data was imported into Progenesis (Nonlinear Dynamics, version 2.0) and processed data was further evaluated using SafeQuant. For database search, the protein database for *M. extorquens* AM1 was downloaded from Uniprot (www.uniprot.org, download date: April 2016; RuBisCO from *R. rubrum* S 1 (Uniprot-ID P04718) was added manually) and search was performed using the decoy strategy. The search criteria were set as follows: full tryptic specificity was required (cleavage after lysine or arginine residues); two missed cleavages were allowed; carbamidomethylation (C) was set as fixed modification; oxidation (M) as variable modification. The mass tolerance was set to 10 ppm for precursor ions and 0.02 Da for fragment ions. The heatmap shown in Fig. 5 was made with GProX (Rigbolt et al., 2011).

2.10. In silico modelling

The *in silico* predictions of the biomass yields were done using flux balance analysis (FBA). To this end, the previously published genome-scale metabolic reconstruction of *M. extorquens* AM1, iRP911, consisting of 1139 reactions and 977 metabolites, was used (Peyraud et al., 2011). To account for the introduced RuBisCO gene, one reaction, representing the conversion of D-Ribulose 1,5-bisphosphate and CO_2 to two molecules of 3-Phospho-D-glycerate, was added to the model. The FBA problem of the form

$$\begin{aligned} &\textbf{\textit{maximize}} && v_{BiomassSynthesis} \\ &\textbf{\textit{subject to}} && S_{ij} * v_j = 0 \\ & && v_j^{lo} \le v_j \le v_j^{up} \end{aligned}$$

where S_{ij} is the stoichiometric matrix and v_j the flux through the reaction *j*, was then implemented using GAMS 2.8.2 and solved using Cplex 12.7.0.0. The lower and upper bounds of v_j were used as specified in iRP911 and only the exchange of O_2, CO_2, H_2O, trace elements (NH_3, Pi, SO_4^{2-}, Na^+, Fe^{2+}, K^+, Mg^{2+}, Cu^{2+}, Mn^{2+}, Zn^{2+}, Cl^-) and the uptake of methanol was allowed.

To realize the knockout mutants, the lower and upper bound of the respective reactions was set to 0. For Δ*glyA*, the reaction R0015 was set to 0, for Δ*ftfL* the reaction R0012 and for Δ*ccr* the reaction R0032. In case of Δ*ftfL* the glycine cleavage complex (R0243/R0244/R0245) and in case of Δ*ccr* the butyryl-CoA carboxylase (R0034) had to be additionally blocked to correctly predict the lethal phenotype, which had been determined in earlier experimental studies (Chistoserdova and Lidstrom, 1996; Marx et al., 2003).

3. Results

3.1. Engineering strategy to realize a synthetic CO_2-fixing M. extorquens AM1 strain

To convert the heterotroph *M. extorquens* AM1 into a synthetic autotroph, we designed an experimental strategy that is based on the decoupling of energy acquisition and carbon assimilation in this organism (Fig. 1). When *M. extorquens* AM1 grows on methanol, 84% of this single carbon compound is completely oxidized to CO_2 to acquire energy, while the remaining 16% of methanol are assimilated into biomass (Fig. 1A) through the serine cycle and a number of interconnected pathways (Peyraud et al., 2011). Deletion of genes essential for methanol assimilation yields mutant strains of *M. extorquens* AM1 that cannot grow on methanol anymore, because they are not able to convert it into biomass. Yet, these mutant strains are still able to draw energy and reducing power from methanol oxidation. When these mutants are equipped with a functional CO_2 fixation pathway, carbon assimilation in *M. extorquens* AM1 should be restored, but from CO_2 and not from reduced organic carbon as in the wild-type (WT) strain, resulting in an autotrophic phenotype (Fig. 1B).

First, we identified several potential target genes of the central carbon metabolism in *M. extorquens* AM1 (see Supplementary Fig. S1)

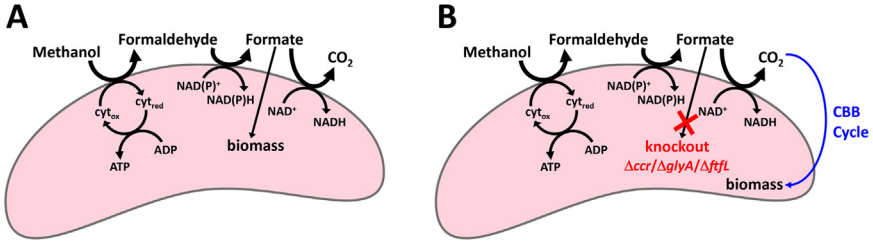

Fig. 1. Engineering strategy for the conversion of *M. extorquens* AM1 into a synthetic autotroph. (A) During WT growth on methanol, this C1 compound is fully oxidized to CO_2 for energy acquisition (i.e., the generation of ATP and reducing equivalents), while carbon for biomass formation is assimilated at the level of formate. (B) In this project, the assimilation of formate is prevented by gene knockouts, so that the cell is forced to utilize CO_2 for biomass formation via the heterologous CBB cycle, while energy acquisition from methanol oxidation still takes place.

that would allow us to largely decouple energy acquisition from carbon assimilation. These included (i) *ccr*, encoding crotonyl-CoA carboxylase/reductase, the key enzyme of the ethylmalonyl-CoA pathway (EMCP) for glyoxylate regeneration (Erb et al., 2007); (ii) *glyA*, encoding serine hydroxymethyltransferase, a key enzyme of the serine cycle (Chistoserdova and Lidstrom, 1994) and (iii) *ftfL*, encoding formate tetrahydrofolate ligase, the enzyme linking methanol oxidation and carbon assimilation (Marx et al., 2003). While the three genes are essential for growth on methanol (Chistoserdova and Lidstrom, 1994, 1996; Marx et al., 2003), the corresponding knock out strains are still able to grow on succinate as carbon source, allowing for genetic manipulations and convenient handling of the corresponding mutants.

To equip *M. extorquens* AM1 with an autotrophic CO_2-fixation module, we decided to implement the CBB cycle in this organism. Of all naturally evolved autotrophic CO_2 fixation pathways (Berg et al., 2010; Fuchs, 2011), the CBB cycle is the one that is most closely connected to proteobacterial central carbon metabolism and requires a minimal number of additional genes to be introduced. Based on genomic analysis, *M. extorquens* AM1 encodes all but one gene of the CBB cycle, namely RuBisCO, so that in principle the heterologous expression of only one protein should be sufficient to establish synthetic autotrophy in this organism.

We used a previously published stoichiometric metabolic network model (Peyraud et al., 2011) and Flux Balance Analysis (FBA) to validate and predict the outcome of this design strategy. Indeed, all three deletion strains (Δ*ccr*, Δ*glyA*, Δ*ftfL*) were predicted to be unable to grow on methanol (see Supplementary Table S3), in line with previously published results for these mutants. Upon implementation of the CBB cycle, the metabolic model predicted recovery of growth on methanol for the *glyA* and *ftfL* deletion strains, but not for the *ccr* deletion strain (see detailed results in Supplementary Table S3). In order to evaluate the output of these *in silico* analyses, we decided to test the three knockout strains as hosts for implementation of the synthetic CBB cycle in *M. extorquens* AM1.

3.2. Realization of a heterologous CBB cycle for CO_2 fixation in M. extorquens AM1

To establish a functional CBB cycle, we first evaluated different RuBisCO candidates for their functionality in *M. extorquens* AM1. We tested a type I RuBisCO from *Paracoccus denitrificans* DSM 413 as well as a type II RuBisCO from *Rhodospirillum rubrum* S 1. Both enzymes had been previously purified and biochemically characterized (Bowien, 1977; Schloss et al., 1979). Moreover, both enzymes are from Alphaproteobacteria closely related to *M. extorquens* AM1, with a similar codon usage and GC content, which makes their heterologous expression in *M. extorquens* AM1 favorable. Plasmid-based expression and solubility of the two enzymes in *M. extorquens* AM1 was confirmed by SDS-PAGE gel analysis (see Supplementary Fig. S2). When assayed in cell extracts of *M. extorquens* AM1, however, only the type II RuBisCO of *R. rubrum* S 1 was active with a specific CO_2 fixation rate of approximately 100 mU/mg total protein. Therefore, we decided to use this enzyme for our heterologous CBB cycle.

Although *M. extorquens* AM1 has a phosphoribulokinase (Prk) homolog encoded in its genome (META1p0758), only very low activity of this enzyme could be measured in extracts of methanol-grown cells (Kalyuzhnaya and Lidstrom, 2003). To realize a sufficiently active CBB cycle we decided to overexpress Prk in addition to RuBisCO. We tested the well-characterized Prk from the cyanobacterium *Synechococcus elongatus* PCC 7942 (Kobayashi et al., 2003), as well as the native homolog from *M. extorquens* AM1. While the cyanobacterial Prk could not be functionally expressed in *M. extorquens* AM1, the native homolog was highly soluble, as judged by SDS-PAGE gel analysis (see Supplementary Fig. S2). Activity of *M. extorquens* AM1 Prk was demonstrated by addition of purified *R. rubrum* S 1 RuBisCO to cell extracts, which allowed us to successfully reconstitute the reaction sequence from ribulose 5-phosphate to glycerate 3-phosphate.

Based on these results, we generated a plasmid-borne carbon fixation module that encoded Prk and RuBisCO in one operon under the control of the strong *mxaF* promoter (Anderson et al., 1990). As negative control for the carbon fixation module, we created a version of the same plasmid encoding Prk as well as a catalytically inactive RuBisCO variant. In this RuBisCO mutant, an essential active site lysine, which is carbamylated in the WT enzyme, was substituted by a methionine, rendering the enzyme inactive (Cleland et al., 1998; Mueller-Cajar et al., 2007). While this RuBisCO active site mutant does not allow for functional CO_2 fixation, it still applies the same burden of protein expression on the host cell, minimizing any epistatic effects. We used this construct as negative control plasmid for all subsequent experiments.

3.3. Screening of M. extorquens AM1 deletion strains with the CBB cycle identifies a distinct phenotype

We next tested the effect of the heterologous CBB cycle in the background of the three mutant strains, Δ*ccr*, Δ*glyA*, and Δ*ftfL*. To this end, the mutant strains were transformed with the plasmid encoding the CBB cycle enzymes RuBisCO and Prk. Precultures were grown on succinate minimal medium, then cells were washed, transferred into methanol minimal medium and the optical density (OD_{600}) of the cultures was monitored over time in 96-well plates.

Under atmospheric CO_2 concentrations, none of the strains tested exhibited an observable phenotype. It is well known that under ambient atmosphere RuBisCO shows a strong side reaction with oxygen that causes accumulation of the toxic compound 2-phosphoglycolate (Bowes et al., 1971). However, when tested in an atmosphere containing 5% CO_2, that effectively suppresses the oxygenase side reaction of RuBisCO, the Δ*ftfL* strain showed a distinct phenotype (Fig. 2). The OD_{600} of Δ*ftfL* carrying the carbon fixation module slowly increased by approximately 50% over the course of about 150 h after transfer into methanol medium, before it stopped. From the increase in OD_{600} during the initial 100 h, we estimated a doubling time of 230 ± 10 h. Notably, neither the Δ*glyA* (in contrast to the *in silico* prediction) nor the Δ*ccr* strains (in agreement with the *in silico* prediction) expressing the CBB cycle, or any of the strains transformed with the empty plasmid or the negative control plasmid with the inactive RuBisCO exhibited this phenotype under the same conditions.

The observed phenotype of the Δ*ftfL* strain overexpressing RuBisCO and Prk was reproducible over many biological replicates ($n > 10$), measured in separate experiments and with different layouts of the 96-well plates in order to exclude any artifacts. However, in several cases, we observed clumping of the cells, which is a well-known problem in *M. extorquens* AM1 liquid cultures (Delaney et al., 2013). Therefore, the *ftfL* deletion was introduced into the previously described Δ*cel* strain that shows a reduced clumping (Delaney et al., 2013). The resulting Δ*cel* Δ*ftfL* double mutant strain was used for all further experiments. In 96-well plate assays, the same phenotype observed for Δ*ftfL* could be reproduced multiple times ($n > 10$) when the Δ*cel* Δ*ftfL* strain was equipped with the carbon fixation module. Again, the observed phenotype was highly reproducible (see Supplementary Fig. S3) and did also not depend on the starting conditions, for example the initial OD_{600} (see Supplementary Fig. S4). A similar phenotype was observed for the same strain when incubated in a bioreactor on methanol medium gassed with 5% CO_2 (see Supplementary Fig. S5). Under these conditions, the increase in OD_{600} ceased after approximately 100 h.

In contrast to the phenotype observed when overexpressing RuBisCO and Prk in the Δ*cel* Δ*ftfL* background, the Δ*cel* strain carrying the same plasmid showed strongly impaired growth on methanol and CO_2 (see Supplementary Fig. S6 and Supplementary Note 1). These experiments demonstrated that a heterologous CBB cycle had a positive effect only in the *M. extorquens* AM1 Δ*cel* Δ*ftfL* background.

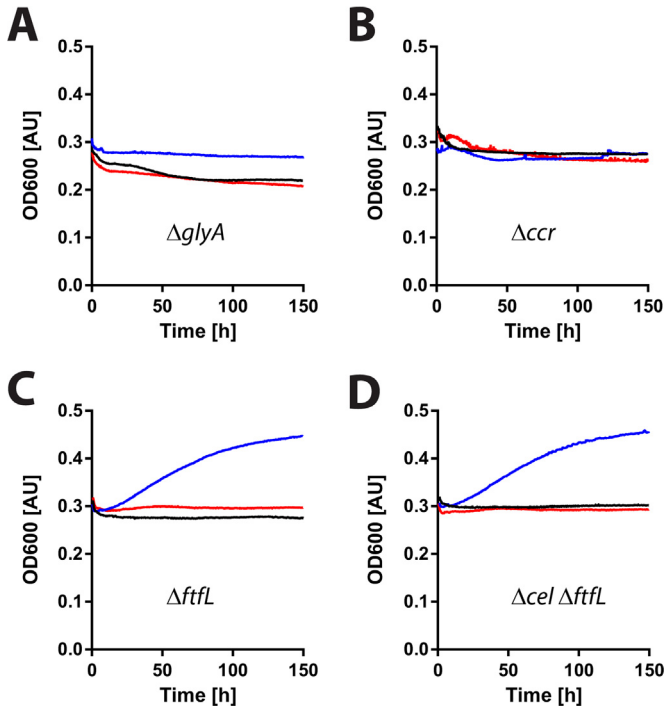

Fig. 2. Growth curves of engineered *M. extorquens* AM1 strains on methanol in a 5% CO_2 atmosphere. The deletion strains of *glyA* (A), *ccr* (B) and *ftfL* (C) are transformed with an empty plasmid backbone (black), a plasmid for the overexpression of RuBisCO and Prk (blue) or a plasmid for the overexpression of catalytically inactive RuBisCO and Prk (red). Growth assays with the double deletion strain Δ*cel* Δ*ftfL* yielded similar results as with Δ*ftfL* (D). Shown are representative curves of at least three technical and at least two biological replicates; for the strains Δ*ftfL* and Δ*cel* Δ*ftfL*, more than 10 biological replicates each were carried out.

3.4. Presence of the CBB cycle increases viability of *M. extorquens* AM1 Δ*cel* Δ*ftfL*

Although the OD_{600} of *M. extorquens* AM1 Δ*cel* Δ*ftfL* expressing the CBB cycle increased on methanol minimal medium with 5% CO_2, the cultures stagnated reproducibly after about 150 h. Transfer in fresh methanol medium did not stimulate a further increase in OD_{600}, independent of whether the transfer took place during the first 150 h or in the stagnation phase (data not shown). Clearly, the Δ*cel* Δ*ftfL* cells engineered with the CBB cycle were not able to sustain continuous growth under these conditions, but seemed to survive longer. Thus, we investigated whether the presence or absence of the heterologous CBB cycle actually correlated to a difference in the number of viable cells.

Because direct cell counting does not yield information about the viability of the cells, we quantified the number of colony forming units (CFU)/mL as a proxy for cell viability. We compared *M. extorquens* AM1 Δ*cel* Δ*ftfL* overexpressing the functional CBB cycle to the negative control that expressed the catalytically inactive RuBisCO. Samples were taken every 50 h, as well as 8 h after inoculation, and plated on agar plates containing succinate minimal medium to quantify viable cells as CFU/mL. While both cultures started from the same initial CFU/mL upon transfer on methanol, the number of viable cells dropped rapidly in the negative control with the non-functional RuBisCO. After 150 h, less than 0.07% of the initial number of CFU/mL were recovered on succinate medium. In contrast, approximately 7% of the initial CFU/mL could be recovered after 150 h for the cells that overexpressed the functional CBB cycle (Fig. 3). The result that not all cells were recovered is in line with the observation that when switching from methanol to succinate medium, only a fraction of cells actively continues to grow (Strovas and Lidstrom, 2009; Strovas et al., 2007). In summary,

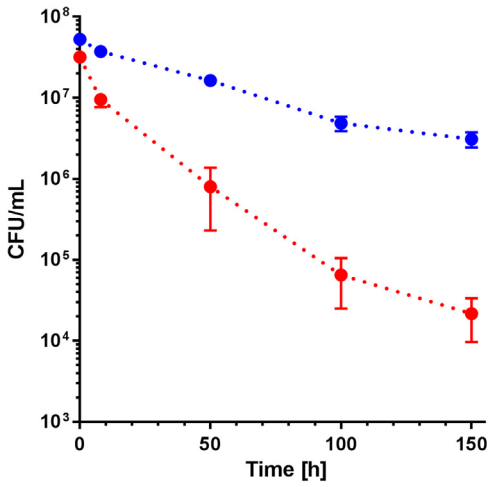

Fig. 3. Time course of CFU/mL during incubation with methanol medium and 5% CO_2. After 150 h, about 100-fold more cells are re-culturable of the strain Δ*cel* Δ*ftfL* with the CBB cycle (blue circles) compared to the negative control strain Δ*cel* Δ*ftfL* with the inactive CBB cycle (red circles). The average of four biological replicates is shown; error bars denote standard deviation.

cells containing a functional carbon fixation module remained more viable by two orders of magnitude compared to the negative control, suggesting that the 100-fold increased viability was directly linked to an actively operating CBB cycle.

3.5. ^{13}C-tracer analysis demonstrates functional CO_2 fixation in *M. extorquens* AM1 via the CBB cycle

Next, we sought to demonstrate functionality of the heterologous CBB cycle by ^{13}C-tracer analysis. For these experiments, *M. extorquens* AM1 Δ*cel* Δ*ftfL* cultures overexpressing either the functional CBB cycle or the negative control were pre-grown in minimal medium containing succinate, washed, and then transferred into minimal medium containing methanol in an atmosphere with 5% CO_2. 4 h after the transfer into methanol medium, aliquots of the cultures were taken and incubated with either ^{13}C-methanol in an atmosphere with 5% non-labeled CO_2, or non-labeled methanol plus ^{13}C-bicarbonate. Then, samples were taken and the time course of ^{13}C-tracer incorporation into metabolites was monitored over 90 min by HPLC-MS. No incorporation of ^{13}C-carbon into metabolites was measured from ^{13}C-methanol in any of the engineered strains (data not shown), confirming that methanol cannot enter central carbon metabolism in the *ftfL* mutant background. When incubated with ^{13}C-bicarbonate, however, we observed incorporation of label into central carbon metabolites in the Δ*cel* Δ*ftfL* strain carrying a functional RuBisCO.

During methylotrophic growth of *M. extorquens* AM1 WT, 50% of carbon is derived from CO_2 that is assimilated via phosphoenolpyruvate (PEP) carboxylase in the serine cycle (Crowther et al., 2008; Large et al., 1961; Peyraud et al., 2011). Notably, CO_2 fixation via PEP carboxylase cannot proceed in the same way in the *ftfL* deletion mutant. Interruption of formate-tetrahydrofolate synthesis prevents continuous operation of the serine cycle, which should result in decreased label incorporation from ^{13}C-bicarbonate via PEP carboxylase. In fact, between 10% and 20% label incorporation into PEP was observed in the *ftfL* mutant background (Fig. 4).

On the other hand, expression of a functional CBB cycle in the background of the *ftfL* mutant should result in the incorporation of bicarbonate-derived ^{13}C-label into CBB cycle metabolites. In agreement with these expectations, we observed ^{13}C-labeled metabolites in the strain engineered with the heterologous CBB cycle. These included phosphoglycerates, pentose mono- and bisphosphates, as well as hexose- and heptose monophosphates, which are all intermediates of

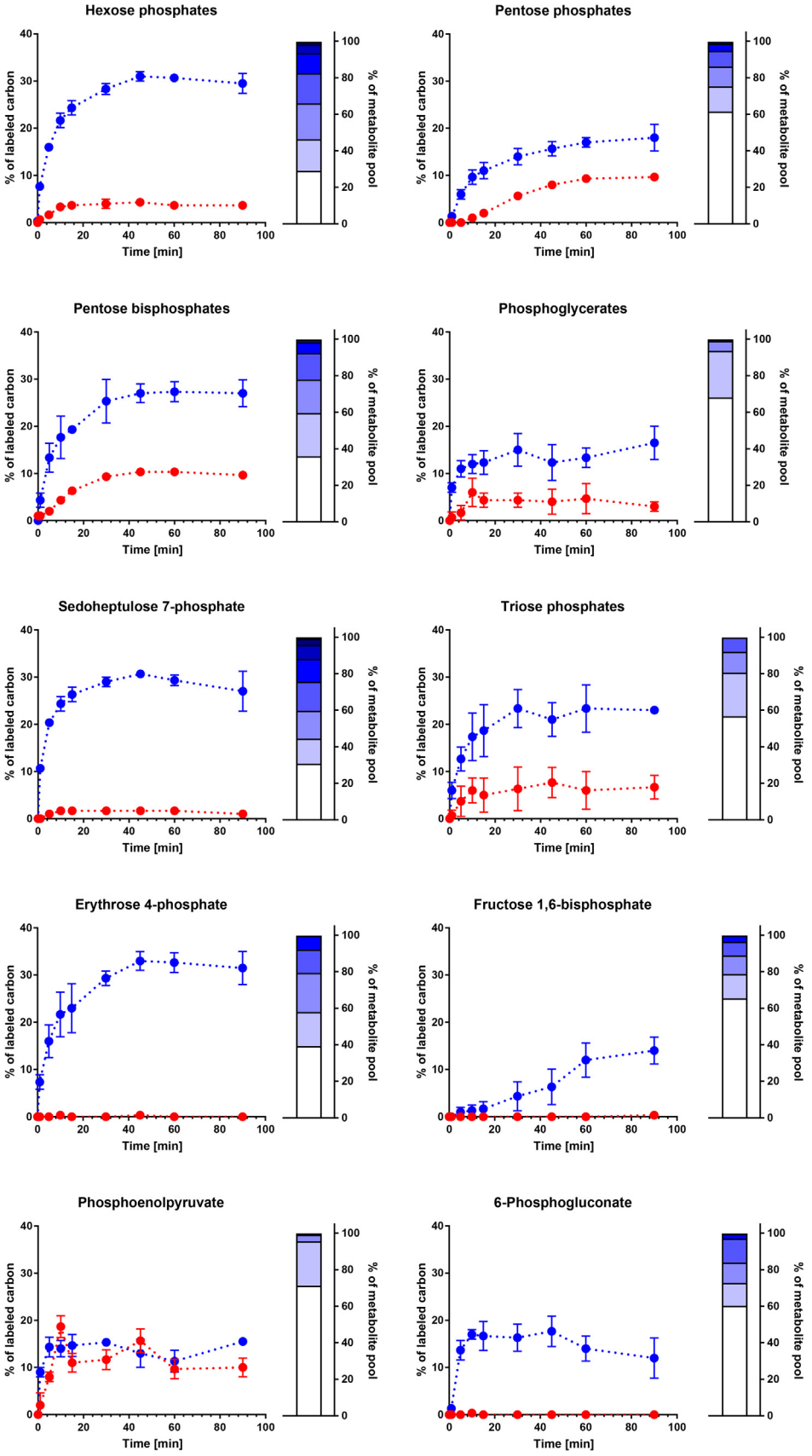

Fig. 4. ^{13}C-tracer analysis in engineered *M. extorquens* AM1 strains with the heterologous CBB cycle from ^{13}C-bicarbonate. ^{13}C-label incorporation in selected metabolites over the course of 90 min is shown 4 h after transfer to minimal medium containing methanol and 5% CO_2. Blue circles: Δ*cel* Δ*ftfL* with the CBB cycle; red circles: Δ*cel* Δ*ftfL* with the inactive CBB cycle. The average of three biological replicates is shown; error bars denote standard deviation. The adjacent bar graphs show the mass isotopologue distribution of the respective metabolite in strain Δ*cel* Δ*ftfL* with the CBB cycle after 60 min incubation with ^{13}C-bicarbonate. The average of three biological replicates is shown; error bars are not shown to increase clarity. Hexose phosphates include glucose 6-phosphate, fructose 6-phosphate and glucose 1-phosphate pools. Pentose phosphates include xylose 5-phosphate, ribose 5-phosphate, xylulose 5-phosphate, and ribulose 5-phosphate pools. Pentose bisphosphates include ribulose 1,5-bisphosphate and ribose 1,5-bisphosphate pools. Phosphoglycerates include 2-phosphoglycerate and 3-phosphoglycerate pools. Triose phosphates include dihydroxyacetone phosphate and glyceraldehyde 3-phosphate pools.

the CBB cycle. Label incorporation proceeded rapidly over the course of the initial 30 min to then become slower and stagnate at 20–30% ^{13}C-labeled carbon for most CBB cycle metabolites (Fig. 4). Notably, fully labeled fractions of all important metabolites of the CBB cycle (e.g., five-fold labeled pentose mono- and bisphosphates, seven-fold labeled sedoheptulose 7-phosphate, etc.) appeared over the course of the

labeling experiment, clearly indicating that the CBB cycle turned multiple times and was active in the strain that carried a functional RuBisCO. The observed labeling patterns and the maximum incorporation of label (20–30%) is in line with results of other studies that also aimed at implementing novel central carbon metabolic features into host organisms, e.g. the engineering of a heterologous ribulose monophosphate cycle in *E. coli* (Müller et al., 2015).

The ^{13}C-tracer incorporation observed in the strain engineered with the heterologous CBB cycle was strongly reduced in the negative control expressing the inactive RuBisCO (Fig. 4). We only observed incorporation into PEP, which is well in line with the residual effect of PEP carboxylase in the interrupted serine cycle. Moreover, we also detected some increasing incorporation of ^{13}C-label into pentose mono- and –bisphosphates. Note that ribulose 1,5-bisphosphate (RuBP) can still be formed in the negative control strain that overexpresses Prk. However, due to inactive RuBisCO, this compound is a metabolic dead end in this strain and accumulates over time. Since RuBP cannot be further metabolized by RuBisCO and is not utilized for biosynthesis, ^{13}C-label in this metabolite can accumulate stronger than in other metabolites, which are drained for biosynthesis or further converted in their respective pathways. With increasing amounts of RuBP being synthesized by Prk, the reaction equilibrium with ribulose 5-phosphate (Ru5P) shifts towards the latter compound, so that ^{13}C-label also accumulates in Ru5P, and, consequently, the pentose phosphate pool. Taken together, the ^{13}C-tracer analysis data strongly suggested that the CBB cycle was operating in the *M. extorquens* AM1 Δ*ftfL* strain equipped with Prk and RuBisCO.

3.6. Comparative proteome analysis reveals specific changes in response to introduction of the CBB cycle

Finally, to identify further adaptions that allowed to establish the observed phenotype we aimed at investigating the effect of the synthetic CBB cycle onto the proteome of *M. extorquens* AM1. To this end, we analyzed the proteome of four different strains upon a substrate switch from succinate to methanol. Our analysis included the *M. extorquens* AM1 Δ*cel* ('wild-type') strain with three engineered variants: Δ*cel* expressing Prk and RuBisCO, Δ*cel* Δ*ftfL* expressing Prk and RuBisCO and Δ*cel* Δ*ftfL* expressing Prk and inactive RuBisCO.

We first grew all strains on succinate and withdrew samples for proteome analysis during exponential phase (succinate condition). Subsequently, we transferred the cells to minimal medium containing methanol as sole carbon source and incubated them in an atmosphere containing 5% CO_2. After a sufficient incubation time (20 h for both of the Δ*cel* strains, 65 h for both of the Δ*cel* Δ*ftfL* strains), we withdrew an additional sample for analysis (methanol condition). We performed whole-cell shotgun proteomics and quantified the change in the proteome of each individual strain in response to the switch from the succinate to the methanol condition (Fig. 5, individual columns). Finally, we compared this data between the four strains. Our analysis identified striking differences in the expression levels of central carbon metabolic enzymes between the four different strains.

It is known that upon switching *M. extorquens* AM1 from succinate to methanol as carbon source, enzymes of the TCA cycle are downregulated, while enzymes of the EMCP become upregulated (Schneider et al., 2012). This pattern was confirmed for the two Δ*cel* strains. In contrast, TCA cycle enzyme expression levels, as well as expression levels of EMCP enzymes did not change in the same way in both Δ*cel* Δ*ftfL* deletion strains during the substrate switch. These changes indicated that the deletion of *ftfL* itself had some general effect on the central carbon metabolism of *M. extorquens* AM1 and that this effect was independent of the presence of an active or inactive CBB cycle.

In addition, PQQ-dependent methanol dehydrogenase and its cytochrome electron acceptor (MxaFGI) are known to be upregulated upon the switch from succinate to methanol (Bosch et al., 2008; Okubo et al., 2007). This pattern was confirmed for both Δ*cel* strains, but notably also the Δ*cel* Δ*ftfL* strain equipped with the active CBB cycle. In contrast, MxaFGI was not upregulated in the strain Δ*cel* Δ*ftfL* carrying the inactive CBB cycle during the substrate switch. This suggests that the *ftfL* deletion strain is able to generate sufficient levels of ATP through methanol oxidation only in the presence of an active CBB cycle, which is in line with the observed phenotype and the increased viability of this strain compared to the inactive CBB cycle control, as described above. The expression levels of RuBisCO and Prk barely decreased between the two sampling time points in both Δ*cel* Δ*ftfL* strains (see Supplementary File 1 for details), indicating that the CBB cycle was active over the course of the whole experiment.

Another striking difference between the four strains was the specific upregulation of a two-subunit transketolase. This enzyme was strongly upregulated only in Δ*cel* Δ*ftfL* carrying the functional CBB cycle, while its expression levels were not significantly influenced by the substrate switch in all other strains. Transketolase is a key enzyme in the CBB cycle for interconversion of sugar phosphates. The specific upregulation of this enzyme in the Δ*cel* Δ*ftfL* strain with the active CBB cycle is expected to increase (or stabilize) flux through the synthetic carbon fixation pathway.

Along the same lines, several enzymes at the beginning of biosynthetic pathways that branch off from the CBB cycle were downregulated only in Δ*cel* Δ*ftfL* expressing the active CBB cycle. This holds true for GlmU, which produces amino sugars from fructose 6-phosphate, PurC and PurK, which operate in the purine biosynthetic pathway that starts from ribose 5-phosphate, RibB, which catalyzes the first step in riboflavin biosynthesis starting from ribulose 5-phosphate, as well as AroG, the enzyme for the first step in the biosynthesis of aromatic amino acids, which utilizes PEP and erythrose 4-phosphate, another metabolite of the CBB cycle, as substrates. The expression levels of all these enzymes in the three other strains were either not significantly changed or barely ($0 > \text{Log2 fold change} > -0.5$) changed upon the switch from succinate to methanol (see Supplementary File 1 for details). The specific downregulation of those five enzymes that drain carbon from the sugar phosphate pools into biosynthesis probably contribute to a more stable operation of the synthetic CBB cycle in the Δ*cel* Δ*ftfL* strain with the functional CBB cycle module. In summary, these experiments identified a specific reaction of the proteome in the presence of an active CBB cycle under selective pressure that explains the observed phenotype and the prolonged viability described above.

4. Discussion

This work aimed at establishing synthetic autotrophy in *M. extorquens* AM1. To that end, we decoupled energy metabolism and carbon assimilation in *M. extorquens* AM1 and equipped the organism with a heterologous CBB cycle. This strategy allowed the organism to acquire energy by methanol oxidation, while it became dependent on CO_2 fixation for biomass synthesis.

To establish a transiently functional CBB cycle for CO_2 fixation, it was sufficient to overexpress only two enzymes in *M. extorquens* AM1 – RuBisCO and Prk. Although *M. extorquens* AM1 encodes an endogenous Prk, this enzyme only performs a regulatory role (Ochsner et al., 2017) and needs to be overexpressed to operate a heterologous CBB cycle in *M. extorquens* AM1. Notably, overexpression of Prk in both the presence and the absence of active RuBisCO was not toxic to *M. extorquens* AM1. This is in stark contrast to *E. coli*, which is known to be sensitive to ribulose 1,5-bisphosphate formation when overexpressing spinach Prk in the absence of RuBisCO (Hudson et al., 1992).

Expression of the CBB cycle in *M. extorquens* AM1 Δ*cel* Δ*ftfL* resulted in a distinct phenotype that strongly increased viability of the engineered cells compared to the negative control. ^{13}C-tracer analysis revealed multiple incorporation of labeled CO_2 into intermediates of the CBB cycle, indicating that the synthetic CO_2 fixation module is indeed functional and can turn multiple times. Proteomics analysis showed distinct changes in the proteome of *M. extorquens* AM1

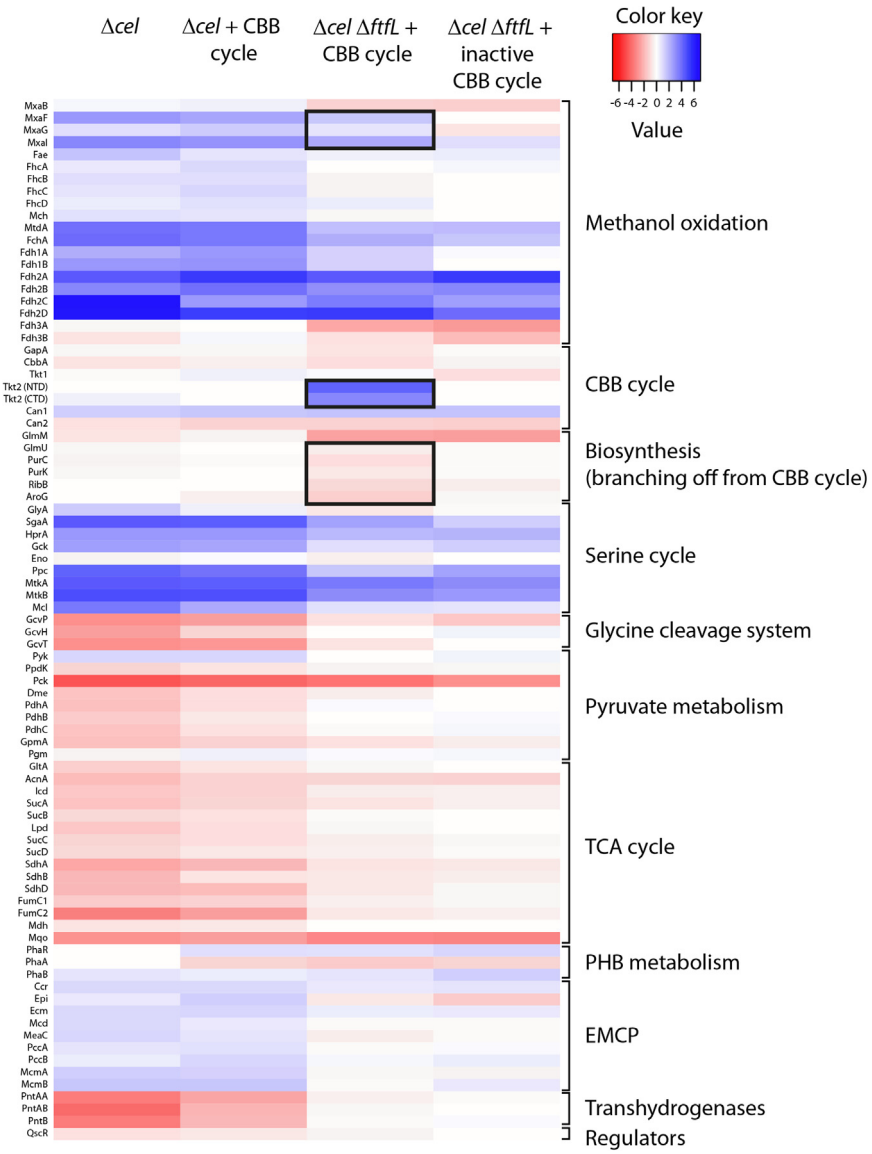

Fig. 5. Whole-cell shotgun proteomics of engineered *M. extorquens* AM1 strains. The heatmap shows the Log2 fold changes in the expression levels of selected proteins upon a substrate switch from succinate to methanol. Proteins that are discussed in the main text are denoted by a black frame. For detailed values and significance of the data see Supplementary File 1.

expressing the functional CBB cycle, which might stabilize flux through the heterologous CO_2 fixation pathway.

While a disruption between methanol oxidation and serine cycle (Δ*ftfL*) can be partially rescued by the heterologous CBB cycle, this is not the case when the metabolic network that is involved in carbon assimilation of tetrahydrofolate-linked C1 units (H_4F-C1) via the serine cycle (Δ*glyA*) or the EMCP (Δ*ccr*) is disrupted. Most likely in the Δ*ftfL* strain the H_4F-C1 units required for biosynthetic pathways can be generated by reverse activity of serine hydroxymethyltransferase (encoded by *glyA*) or by operation of the glycine cleavage complex. In contrast, the *glyA* deletion strain would require a horse shoe-like operation of the serine cycle together with the glycine cleavage complex to generate serine, glycine and H_4F-C1 units. Although predicted to be viable with a carbon fixation pathway by *in silico* analysis, this metabolic mode is apparently not supported by a *glyA* deletion strain expressing a heterologous CBB cycle. Similarly, interruption of glyoxylate regeneration caused by deletion of *ccr* cannot be compensated by the heterologous CBB cycle, probably because the heterologous CBB cycle cannot provide sufficient precursors for synthesis of glyoxylate and subsequently of glycine and serine.

Despite the promising results obtained in this study, no continuous growth of strains engineered with the CBB cycle could be observed on methanol and CO_2 thus far. A major challenge in establishing synthetic metabolic cycles is to delicately balance the continuous operation of a cycle with the requirement to constantly drain metabolites from the cycle into biosynthetic pathways (Barenholz et al., 2017). Too little flux into biosynthesis will slow down growth, while too much flux into biosynthetic routes will inevitably bring the cycle to a hold. These problems were also identified in recent efforts that aimed at establishing artificial methylotrophy in *E. coli* (Müller et al., 2015), as well as implementing a heterologous CBB cycle for sugar synthesis from CO_2 in *E. coli* (Antonovsky et al., 2016). For the latter, it was demonstrated that a reduced catalytic capacity of enzymes that drain intermediates from the CBB cycle into biosynthesis was a key factor in establishing a stably operating heterologous CBB cycle in *E. coli* (Herz et al., 2017). The same challenge of balancing metabolic fluxes exists in the case of engineering a heterologous CBB cycle in *M. extorquens* AM1. A sufficient pool of ribulose 1,5-bisphosphate needs to be maintained to ensure continuous carbon fixation, while at the same time precursors need to be drained for biomass formation (see Supplementary Fig. S7). Along these lines, it

is interesting to note that we observed a specific upregulation of enzymes that increase flux and a specific downregulation of enzymes that drain intermediates from the CBB cycle upon expression of Prk and RuBisCO in *M. extorquens* AM1. However, these changes in enzyme expression levels do not seem to be sufficient to sustain a long-lasting operation of the heterologous carbon fixation pathway. An obvious next step towards sustained growth of our engineered organism would be to improve flux through the synthetic CBB cycle by rational approaches as well as by directed evolution, in a similar way as described (Antonovsky et al., 2016), with a special focus on mutations that decrease the catalytic capacity of enzymes that affect the efflux of CBB cycle metabolites from the autocatalytic carbon fixation pathway towards biosynthesis (Herz et al., 2017).

In summary, our study represents another step forward in the generation of synthetic autotrophic organisms by rational metabolic engineering. Using *M. extorquens* AM1, a platform organism for a future C1 bioindustry, we could demonstrate that it is in principle possible to completely separate energy metabolism and carbon assimilation in this bacterium to create a synthetic organoautotroph that can use the C1 carbon source methanol for energy acquisition, but is dependent on CO_2 for the formation of biomass. Our results open the possibility to further improve synthetic autotrophy in *M. extorquens* AM1. At the same time, they lay the foundation for further explorations of the modularity of our approach. For instance, instead of the CBB cycle a non-natural carbon fixation pathway (Bar-Even et al., 2010; Schwander et al., 2016) could be introduced into *M. extorquens* AM1. Furthermore, replacing methanol as energy source with hydrogen, light or electricity could allow to create versatile synthetic autotrophs for biotechnology in the future.

Acknowledgements

We are grateful to Philipp Christen for skillful assistance with LC-MS sample measurement, to Andreas Kautz for help with running bioreactors and to Ryan Farmer and Bob Tabita for kindly providing purified RuBisCO from *R. rubrum* S 1. We are greatly indebted to Julia A. Vorholt for hosting the project in her laboratory at ETH Zurich during its initial stages as well as for helpful discussions.

Funding

This work was supported by ETH Zurich Grant ETH-41/12-2, an IMPRS fellowship for M.C., and the Max Planck Society.

Author contributions

T.J.E. conceived the project; L.S.v.B. and T.J.E. designed research, analyzed data and wrote the manuscript with input from all authors; L.S.v.B., M.C. and R.W. performed the experiments; T.G. performed LC-MS measurements for proteomics and analyzed the data; P.K. performed LC-MS measurements for metabolic tracer analysis and provided advice and resources for data analysis; and S.L. and M.H. performed *in silico* analyses.

Competing financial interests

The authors declare no competing financial interests.

Appendix A. Supplementary material

Supplementary data associated with this article can be found in the online version at http://dx.doi.org/10.1016/j.ymben.2018.04.003.

References

Ahrné, E., Molzahn, L., Glatter, T., Schmidt, A., 2013. Critical assessment of proteome-wide label-free absolute abundance estimation strategies. Proteomics 13, 2567–2578.

Anderson, D.J., Morris, C.J., Nunn, D.N., Anthony, C., Lidstrom, M.E., 1990. Nucleotide sequence of the *Methylobacterium extorquens* AM1 *moxF* and *moxJ* genes involved in methanol oxidation. Gene 90, 173–176.

Antonovsky, N., Gleizer, S., Noor, E., Zohar, Y., Herz, E., Barenholz, U., Zelcbuch, L., Amram, S., Wides, A., Tepper, N., Davidi, D., Bar-On, Y., Bareia, T., Wernick, D.G., Shani, I., Malitsky, S., Jona, G., Bar-Even, A., Milo, R., 2016. Sugar synthesis from CO_2 in *Escherichia coli*. Cell 166, 115–125.

Bar-Even, A., Noor, E., Lewis, N.E., Milo, R., 2010. Design and analysis of synthetic carbon fixation pathways. Proc. Natl. Acad. Sci. USA 107, 8889–8894.

Barenholz, U., Davidi, D., Reznik, E., Bar-On, Y., Antonovsky, N., Noor, E., Milo, R., 2017. Design principles of autocatalytic cycles constrain enzyme kinetics and force low substrate saturation at flux branch points. eLife 6.

Berg, I.A., Kockelkorn, D., Ramos-Vera, W.H., Say, R.F., Zarzycki, J., Hugler, M., Alber, B.E., Fuchs, G., 2010. Autotrophic carbon fixation in archaea. Nat. Rev. Microbiol. 8, 447–460.

Bertau, M., Offermanns, H., Plass, L., Schmidt, F., Wernicke, H.-J., 2014. Methanol: The Basic Chemical and Energy Feedstock of the Future. Springer-Verlag, Berlin, Heidelberg.

Bosch, G., Skovran, E., Xia, Q., Wang, T., Taub, F., Miller, J.A., Lidstrom, M.E., Hackett, M., 2008. Comprehensive proteomics of *Methylobacterium extorquens* AM1 metabolism under single carbon and nonmethylotrophic conditions. Proteomics 8, 3494–3505.

Bowes, G., Ogren, W.L., Hageman, R.H., 1971. Phosphoglycolate production catalyzed by ribulose diphosphate carboxylase. Biochem. Biophys. Res. Commun. 45, 716–722.

Bowien, B., 1977. D-ribulose 1,5-bisphosphate carboxylase from *Paracoccus denitrificans*. FEMS Microbiol. Lett. 2, 263–266.

Bradford, M.M., 1976. A rapid and sensitive method for the quantitation of microgram quantities of protein utilizing the principle of protein-dye binding. Anal. Biochem. 72, 248–254.

Chistoserdova, L.V., Lidstrom, M.E., 1994. Genetics of the serine cycle in *Methylobacterium extorquens* AM1: cloning, sequence, mutation, and physiological effect of *glyA*, the gene for serine hydroxymethyltransferase. J. Bacteriol. 176, 6759–6762.

Chistoserdova, L.V., Lidstrom, M.E., 1996. Molecular characterization of a chromosomal region involved in the oxidation of acetyl-CoA to glyoxylate in the isocitrate-lyase-negative methylotroph *Methylobacterium extorquens* AM1. Microbiology 142, 1459–1468.

Choi, Y.J., Morel, L., Bourque, D., Mullick, A., Massie, B., Miguez, C.B., 2006. Bestowing inducibility on the cloned methanol dehydrogenase promoter (*P*mxaF) of *Methylobacterium extorquens* by applying regulatory elements of *Pseudomonas putida* F1. Appl. Environ. Microbiol. 72, 7723–7729.

Chubiz, L.M., Purswani, J., Carroll, S.M., Marx, C.J., 2013. A novel pair of inducible expression vectors for use in *Methylobacterium extorquens*. BMC Res. Notes 6, 183.

Cleland, W.W., Andrews, T.J., Gutteridge, S., Hartman, F.C., Lorimer, G.H., 1998. Mechanism of RuBisCO: the carbamate as general base. Chem. Rev. 98, 549–562.

Crowther, G.J., Kosaly, G., Lidstrom, M.E., 2008. Formate as the main branch point for methylotrophic metabolism in *Methylobacterium extorquens* AM1. J. Bacteriol. 190, 5057–5062.

Delaney, N.F., Kaczmarek, M.E., Ward, L.M., Swanson, P.K., Lee, M.C., Marx, C.J., 2013. Development of an optimized medium, strain and high-throughput culturing methods for *Methylobacterium extorquens*. PLoS One 8, e62957.

Dellomonaco, C., Clomburg, J.M., Miller, E.N., Gonzalez, R., 2011. Engineered reversal of the beta-oxidation cycle for the synthesis of fuels and chemicals. Nature 476, 355–359.

Enquist-Newman, M., Faust, A.M., Bravo, D.D., Santos, C.N., Raisner, R.M., Hanel, A., Sarvabhowman, P., Le, C., Regitsky, D.D., Cooper, S.R., Peereboom, L., Clark, A., Martinez, Y., Goldsmith, J., Cho, M.Y., Donohoue, P.D., Luo, L., Lamberson, B., Tamrakar, P., Kim, E.J., Villari, J.L., Gill, A., Tripathi, S.A., Karamchedu, P., Paredes, C.J., Rajgarhia, V., Kotlar, H.K., Bailey, R.B., Miller, D.J., Ohler, N.L., Swimmer, C., Yoshikuni, Y., 2014. Efficient ethanol production from brown macroalgae sugars by a synthetic yeast platform. Nature 505, 239–243.

Erb, T.J., Berg, I.A., Brecht, V., Müller, M., Fuchs, G., Alber, B.E., 2007. Synthesis of C5-dicarboxylic acids from C2-units involving crotonyl-CoA carboxylase/reductase: the ethylmalonyl-CoA pathway. Proc. Natl. Acad. Sci. USA 104, 10631–10636.

Fargione, J., Hill, J., Tilman, D., Polasky, S., Hawthorne, P., 2008. Land clearing and the biofuel carbon debt. Science 319, 1235–1238.

Fuchs, G., 2011. Alternative pathways of carbon dioxide fixation: insights into the early evolution of life? Annu. Rev. Microbiol. 65, 631–658.

Galanie, S., Thodey, K., Trenchard, I.J., Filsinger Interrante, M., Smolke, C.D., 2015. Complete biosynthesis of opioids in yeast. Science 349, 1095–1100.

Glatter, T., Ahrné, E., Schmidt, A., 2015. Comparison of different sample preparation protocols reveals lysis buffer-specific extraction biases in gram-negative bacteria and human cells. J. Proteome Res. 14, 4472–4485.

Herz, E., Antonovsky, N., Bar-On, Y., Davidi, D., Gleizer, S., Prywes, N., Noda-Garcia, L., Lyn Frisch, K., Zohar, Y., Wernick, D.G., Savidor, A., Barenholz, U., Milo, R., 2017. The genetic basis for the adaptation of *E. coli* to sugar synthesis from CO_2. Nat. Commun. 8, 1705.

Hofer, P., Choi, Y.J., Osborne, M.J., Miguez, C.B., Vermette, P., Groleau, D., 2010. Production of functionalized polyhydroxyalkanoates by genetically modified *Methylobacterium extorquens* strains. Microb. Cell Fact. 9, 70.

Hu, B., Lidstrom, M.E., 2014. Metabolic engineering of *Methylobacterium extorquens* AM1 for 1-butanol production. Biotechnol. Biofuels 7, 156.

Hudson, G.S., Morell, M.K., Arvidsson, Y.B.C., Andrews, T.J., 1992. Synthesis of spinach phosphoribulokinase and ribulose 1,5-bisphosphate in *Escherichia coli*. Aust. J. Plant Physiol. 19, 213–221.

Kalyuzhnaya, M.G., Lidstrom, M.E., 2003. QscR, a LysR-type transcriptional regulator and

CbbR homolog, is involved in regulation of the serine cycle genes in *Methylobacterium extorquens* AM1. J. Bacteriol. 185, 1229–1235.
Kiefer, P., Schmitt, U., Vorholt, J.A., 2013. eMZed: an open source framework in Python for rapid and interactive development of LC/MS data analysis workflows. Bioinformatics 29, 963–964.
Kobayashi, D., Tamoi, M., Iwaki, T., Shigeoka, S., Wadano, A., 2003. Molecular characterization and redox regulation of phosphoribulokinase from the cyanobacterium *Synechococcus* sp. PCC 7942. Plant Cell Physiol. 44, 269–276.
Laemmli, U.K., 1970. Cleavage of structural proteins during the assembly of the head of bacteriophage T4. Nature 227, 680–685.
Large, P.J., Peel, D., Quayle, J.R., 1961. Microbial growth on C1 compounds. 2. Synthesis of cell constituents by methanol- and formate-grown *Pseudomonas* AM 1, and methanol-grown *Hyphomicrobium vulgare*. Biochem. J. 81, 470–480.
Liu, C., Colon, B.C., Ziesack, M., Silver, P.A., Nocera, D.G., 2016. Water splitting-biosynthetic system with CO_2 reduction efficiencies exceeding photosynthesis. Science 352, 1210–1213.
Marx, C.J., 2008. Development of a broad-host-range *sacB*-based vector for unmarked allelic exchange. BMC Res. Notes 1, 1.
Marx, C.J., Laukel, M., Vorholt, J.A., Lidstrom, M.E., 2003. Purification of the formate-tetrahydrofolate ligase from *Methylobacterium extorquens* AM1 and demonstration of its requirement for methylotrophic growth. J. Bacteriol. 185, 7169–7175.
Marx, C.J., Lidstrom, M.E., 2001. Development of improved versatile broad-host-range vectors for use in methylotrophs and other gram-negative bacteria. Microbiology 147, 2065–2075.
Marx, C.J., Lidstrom, M.E., 2002. Broad-host-range *cre-lox* system for antibiotic marker recycling in gram-negative bacteria. BioTechniques 33, 1062–1067.
Marx, C.J., Lidstrom, M.E., 2004. Development of an insertional expression vector system for *Methylobacterium extorquens* AM1 and generation of null mutants lacking *mtdA* and/or *fch*. Microbiology 150, 9–19.
Mattozzi, M.D., Ziesack, M., Voges, M.J., Silver, P.A., Way, J.C., 2013. Expression of the sub-pathways of the *Chloroflexus aurantiacus* 3-hydroxypropionate carbon fixation bicycle in *E. coli*: Toward horizontal transfer of autotrophic growth. Metab. Eng. 16, 130–139.
Mueller-Cajar, O., Morell, M., Whitney, S.M., 2007. Directed evolution of RuBisCO in *Escherichia coli* reveals a specificity-determining hydrogen bond in the form II enzyme. Biochemistry 46, 14067–14074.
Müller, J.E.N., Meyer, F., Litsanov, B., Kiefer, P., Potthoff, E., Heux, S., Quax, W.J., Wendisch, V.F., Brautaset, T., Portais, J.C., Vorholt, J.A., 2015. Engineering *Escherichia coli* for methanol conversion. Metab. Eng. 28, 190–201.
Nichols, E.M., Gallagher, J.J., Liu, C., Su, Y., Resasco, J., Yu, Y., Sun, Y., Yang, P., Chang, M.C., Chang, C.J., 2015. Hybrid bioinorganic approach to solar-to-chemical conversion. Proc. Natl. Acad. Sci. USA 112, 11461–11466.
Ochsner, A.M., Christen, M., Hemmerle, L., Peyraud, R., Christen, B., Vorholt, J.A., 2017. Transposon sequencing uncovers an essential regulatory function of phosphoribulokinase for methylotrophy. Curr. Biol. 27, 2579–2588.
Ochsner, A.M., Sonntag, F., Buchhaupt, M., Schrader, J., Vorholt, J.A., 2015. *Methylobacterium extorquens*: methylotrophy and biotechnological applications. Appl. Microbiol. Biotechnol. 99, 517–534.
Okubo, Y., Skovran, E., Guo, X., Sivam, D., Lidstrom, M.E., 2007. Implementation of microarrays for *Methylobacterium extorquens* AM1. Omics 11, 325–340.
Olah, G.A., 2013. Towards oil independence through renewable methanol chemistry. Angew. Chem. Int. Ed. 52, 104–107.
Orita, I., Nishikawa, K., Nakamura, S., Fukui, T., 2014. Biosynthesis of polyhydroxyalkanoate copolymers from methanol by *Methylobacterium extorquens* AM1 and the engineered strains under cobalt-deficient conditions. Appl. Microbiol. Biotechnol. 98, 3715–3725.
Paddon, C.J., Westfall, P.J., Pitera, D.J., Benjamin, K., Fisher, K., McPhee, D., Leavell, M.D., Tai, A., Main, A., Eng, D., Polichuk, D.R., Teoh, K.H., Reed, D.W., Treynor, T., Lenihan, J., Fleck, M., Bajad, S., Dang, G., Dengrove, D., Diola, D., Dorin, G., Ellens, K.W., Fickes, S., Galazzo, J., Gaucher, S.P., Geistlinger, T., Henry, R., Hepp, M., Horning, T., Iqbal, T., Jiang, H., Kizer, L., Lieu, B., Melis, D., Moss, N., Regentin, R., Secrest, S., Tsuruta, H., Vazquez, R., Westblade, L.F., Xu, L., Yu, M., Zhang, Y., Zhao, L., Lievense, J., Covello, P.S., Keasling, J.D., Reiling, K.K., Renninger, N.S., Newman, J.D., 2013. High-level semi-synthetic production of the potent antimalarial artemisinin. Nature 496, 528–532.
Peel, D., Quayle, J.R., 1961. Microbial growth on C1 compounds. 1. Isolation and characterization of *Pseudomonas* AM 1. Biochem. J. 81, 465–469.
Peyraud, R., Kiefer, P., Christen, P., Massou, S., Portais, J.C., Vorholt, J.A., 2009. Demonstration of the ethylmalonyl-CoA pathway by using ^{13}C metabolomics. Proc. Natl. Acad. Sci. USA 106, 4846–4851.
Peyraud, R., Schneider, K., Kiefer, P., Massou, S., Vorholt, J.A., Portais, J.C., 2011. Genome-scale reconstruction and system level investigation of the metabolic network of *Methylobacterium extorquens* AM1. BMC Syst. Biol. 5, 189.
Racker, E., 1957. The reductive pentose phosphate cycle. I. Phosphoribulokinase and ribulose diphosphate carboxylase. Arch. Biochem. Biophys. 69, 300–310.
Racker, E., 1962. Ribulose diphosphate carboxylase from spinach leaves. Method. Enzymol. 5, 266–270.
Rigbolt, K.T., Vanselow, J.T., Blagoev, B., 2011. GProX, a user-friendly platform for bioinformatics analysis and visualization of quantitative proteomics data. Mol. Cell. Proteom. 10 (O110.007450).
Sambrook, J., Russell, D.W., 2001. Molecular Cloning: A Laboratory Manual. Cold Spring Harbor Laboratory Press, Cold Spring Harbor, NY.
Schada von Borzyskowski, L., Remus-Emsermann, M., Weishaupt, R., Vorholt, J.A., Erb, T.J., 2015. A set of versatile brick vectors and promoters for the assembly, expression, and integration of synthetic operons in *Methylobacterium extorquens* AM1 and other Alphaproteobacteria. ACS Synth. Biol. 4, 430–443.
Schäfer, A., Tauch, A., Jäger, W., Kalinowski, J., Thierbach, G., Pühler, A., 1994. Small mobilizable multi-purpose cloning vectors derived from the *Escherichia coli* plasmids pK18 and pK19: selection of defined deletions in the chromosome of *Corynebacterium glutamicum*. Gene 145, 69–73.
Schloss, J.V., Phares, E.F., Long, M.V., Norton, I.L., Stringer, C.D., Hartman, F.C., 1979. Isolation, characterization, and crystallization of ribulose bisphosphate carboxylase from autotrophically grown *Rhodospirillum rubrum*. J. Bacteriol. 137, 490–501.
Schneider, K., Peyraud, R., Kiefer, P., Christen, P., Delmotte, N., Massou, S., Portais, J.C., Vorholt, J.A., 2012. The ethylmalonyl-CoA pathway is used in place of the glyoxylate cycle by *Methylobacterium extorquens* AM1 during growth on acetate. J. Biol. Chem. 287, 757–766.
Schrader, J., Schilling, M., Holtmann, D., Sell, D., Filho, M.V., Marx, A., Vorholt, J.A., 2009. Methanol-based industrial biotechnology: current status and future perspectives of methylotrophic bacteria. Trends Biotechnol. 27, 107–115.
Schwander, T., Schada von Borzyskowski, L., Burgener, S., Cortina, N.S., Erb, T.J., 2016. A synthetic pathway for the fixation of carbon dioxide *in vitro*. Science 354, 900–904.
Sims, R.E., Mabee, W., Saddler, J.N., Taylor, M., 2010. An overview of second generation biofuel technologies. Bioresour. Technol. 101, 1570–1580.
Sonntag, F., Buchhaupt, M., Schrader, J., 2014. Thioesterases for ethylmalonyl-CoA pathway-derived dicarboxylic acid production in *Methylobacterium extorquens* AM1. Appl. Microbiol. Biotechnol. 98, 4533–4544.
Sonntag, F., Kroner, C., Lubuta, P., Peyraud, R., Horst, A., Buchhaupt, M., Schrader, J., 2015a. Engineering *Methylobacterium extorquens* for *de novo* synthesis of the sesquiterpenoid alpha-humulene from methanol. Metab. Eng. 32, 82–94.
Sonntag, F., Müller, J.E.N., Kiefer, P., Vorholt, J.A., Schrader, J., Buchhaupt, M., 2015b. High-level production of ethylmalonyl-CoA pathway-derived dicarboxylic acids by *Methylobacterium extorquens* under cobalt-deficient conditions and by polyhydroxybutyrate negative strains. Appl. Microbiol. Biotechnol. 99, 3407–3419.
Strovas, T.J., Lidstrom, M.E., 2009. Population heterogeneity in *Methylobacterium extorquens* AM1. Microbiology 155, 2040–2048.
Strovas, T.J., Sauter, L.M., Guo, X., Lidstrom, M.E., 2007. Cell-to-cell heterogeneity in growth rate and gene expression in *Methylobacterium extorquens* AM1. J. Bacteriol. 189, 7127–7133.
Toyama, H., Anthony, C., Lidstrom, M.E., 1998. Construction of insertion and deletion *mxa* mutants of *Methylobacterium extorquens* AM1 by electroporation. FEMS Microbiol. Lett. 166, 1–7.
Zhuang, Z.Y., Li, S.Y., 2013. RuBisCO-based engineered *Escherichia coli* for *in situ* carbon dioxide recycling. Bioresour. Technol. 150, 79–88.